Journal of Immunological Methods 475 (2019) 112662

Contents lists available at ScienceDirect

Journal of Immunological Methods

journal homepage: www.elsevier.com/locate/jim

Research paper

EuroFlow Lymphoid Screening Tube (LST) data base for automated identification of blood lymphocyte subsets

Juan Flores-Montero[a,1], Georgiana Grigore[b,1], Rafael Fluxá[b], Juan Hernández[b], Paula Fernandez[c], Julia Almeida[a], Noemí Muñoz[a], Sebastian Böttcher[d], Lukasz Sedek[e], Vincent van der Velden[f], Susana Barrena[a], Alejando Hernández[a], Bruno Paiva[g], Quentin Lecrevisse[a], Margarida Lima[h], Ana Helena Santos[h], Jacques J.M. van Dongen[i,**], Alberto Orfao[a,*]

[a] Cancer Research Center (IBMCC-CSIC/USAL-IBSAL); Cytometry Service (NUCLEUS) and Department of Medicine, University of Salamanca, Salamanca, Spain and; Centro de Investigación Biomédica en Red de Cáncer: CIBER-ONC (CB16/12/00400), Instituto de Salud Carlos III, Madrid, Spain
[b] Cytognos SL, Salamanca, Spain
[c] FACS/Stem cell Laboratory, Institute of Laboratory Medicine, Kantonsspital Aarau AG, Aarau, Switzerland
[d] Division of Internal Medicine, Medical Clinic III, Hematology, Oncology and Palliative Medicine, Special Hematology Laboratory, Rostock University Medical Center, Rostock, Germany
[e] Department of Pediatric Hematology and Oncology, Medical University of Silesia in Katowice, Zabrze, Poland
[f] Department of Immunology, Erasmus MC, Erasmus University Medical Center, Rotterdam, the Netherlands
[g] Clínica Universidad de Navarranica, CIMA, IDISNA, CIBERONC CB16/12/00369, Pamplona, Spain
[h] Department of Hematology, Laboratory of Cytometry, Hospital de Santo António, Centro Hospitalar do Porto, and Unit for Multidisciplinary Research in Biomedicine (UMIB), Porto, Portugal
[i] Department of Immunohematology and Blood Transfusion, Leiden University Medical Center, Leiden, the Netherlands

A B S T R A C T

In recent years the volume and complexity of flow cytometry data has increased substantially. This has led to a greater number of identifiable cell populations in a single measurement. Consequently, new gating strategies and new approaches for cell population definition are required. Here we describe how the EuroFlow Lymphoid Screening Tube (LST) reference data base for peripheral blood (PB) samples was designed, constructed and validated for automated gating of the distinct lymphoid (and myeloid) subsets in PB of patients with chronic lymphoproliferative disorders (CLPD). A total of 46 healthy/reactive PB samples which fulfilled predefined technical requirements, were used to construct the LST-PB reference data base. In addition, another set of 92 PB samples (corresponding to 10 healthy subjects, 51 B-cell CLPD and 31 T/NK-cell CLPD patients), were used to validate the automated gating and cell-population labeling tools with the Infinicyt software.

An overall high performance of the LST-PB data base was observed with a median percentage of alarmed cellular events of 0.8% in 10 healthy donor samples and of 44.4% in CLPD data files containing 49.8% (range: 1.3–96%) tumor cells. The higher percent of alarmed cellular events in every CLPD sample was due to aberrant phenotypes (75.6% cases) and/or to abnormally increased cell counts (86.6% samples). All 18 (22%) data files that only displayed numerical alterations, corresponded to T/NK-cell CLPD cases which showed a lower incidence of aberrant phenotypes (41%) vs B-cell CLPD cases (100%). Comparison between automated vs expert-bases manual classification of normal ($r^2 = 0.96$) and tumor cell populations (*rho* = 0.99) showed a high degree of correlation.

In summary, our results show that automated gating of cell populations based on the EuroFlow LST-PB data base provides an innovative, reliable and reproducible tool for fast and simplified identification of normal vs pathological B and T/NK lymphocytes in PB of CLPD patients.

1. Introduction

Multiparameter flow cytometry has become the method of choice for phenotypic characterization of normal and pathological blood and immune cell populations, particularly in the field of hemato-oncology (Johansson et al., 2014; Leach et al., 2013; Matarraz et al., 2017; Paiva et al., 2016; Swerdlow et al., 2008; van Dongen et al., 2012) and primary immunodeficiencies (Blanco et al., 2019; O'Gorman et al., 2011; van der Burg et al., 2019). This has been strongly facilitated by: i) an increased number of phenotypic markers available to investigate blood

* Correspondence to: Alberto Orfao, Centro de Investigación del Cáncer (CSIC-USAL), Avda. Universidad de Coimbra S/N, Campus Miguel de Unamuno, Salamanca 37007, Spain.
** Correspondence to: Jacques J.M. van Dongen, Department of Immunohematology and Blood Transfusion, Leiden University Medical Center, Albinusdreef 2, 2333 ZA, Leiden, The Netherlands.
E-mail addresses: J.J.M.van_Dongen@lumc.nl (J.J.M. van Dongen), orfao@usal.es (A. Orfao).
[1] These authors have equally contributed to this work.

https://doi.org/10.1016/j.jim.2019.112662
Received 4 April 2019; Received in revised form 31 July 2019; Accepted 22 August 2019
Available online 24 August 2019

and immune cells (Engel et al., 2015); ii) availability of greater numbers and high-quality antibody clones and fluorochrome conjugates (Flores-Montero et al., 2019) and; iii) development of flow cytometry instruments capable of simultaneously analyzing more fluorochromes and greater numbers of cells at a faster rate (Chattopadhyay et al., 2019). These advances have generated higher volumes of data that require subsequent analysis and interpretation by experts.

In the context of hemato-oncology, such analyses, should not only focus on the aberrant target cell populations, but also on residual normal cells. Because of the possibility to identify tens to hundreds of cell populations in a single measurement, classical expert-guided manual gating strategies based on the identification of each individual cell population via bivariate dot plots (i.e. Boolean gating strategy), has become suboptimal in routine diagnostics. The complexity of conventional gating approaches requires a significant amount of knowledge, expertise and time for accurate interpretation of the many coexisting normal and abnormal cell phenotypes (Heel et al., 2013; Pedreira et al., 2013; Saeys et al., 2016). In addition, such complex expert-based manual gating approach suffers from greater levels of subjectivity and consequently higher variability. Therefore, it would be attractive to develop automated gating strategies, that allow accurate and reproducible identification of distinct normal and aberrant cell populations coexisting in a sample in routine clinical flow cytometry diagnostics (Johansson et al., 2014; Pedreira et al., 2019; Workgroup, 2013).

In recent years, several automated gating approaches with multiple clustering algorithms have been proposed for identification of distinct groups of events coexisting in a sample (Chester and Maecker, 2015; Meehan et al., 2014; O'Neill et al., 2013; Pedreira et al., 2008a, 2013; Petrausch et al., 2006; Saeys et al., 2016). However, only a few have addressed automated classification of such groups of events as biologically meaningful cell populations, and none of the automated gating strategies has been clinically validated in large patient series (Chester and Maecker, 2015; Meehan et al., 2014; O'Neill et al., 2013; Saeys et al., 2016). In order to overcome the above limitations, EuroFlow (a scientific consortium aiming at standardization and innovation in flow cytometry)(van Dongen and Orfao, 2012) has developed new data bases of fully annotated flow cytometry data files from normal and pathological samples stained with EuroFlow screening tubes and antibody panels (Flores-Montero et al., 2017; Pedreira et al., 2019; Theunissen et al., 2016; van der Burg et al., 2019; van Dongen et al., 2012). Comparison of groups of events obtained by automated gating clustering algorithms against such data bases, allows their unequivocal classification into cell populations with a biological and/or clinical meaning (Pedreira et al., 2019). Automated identification of the major and minor cell populations coexisting in a flow cytometric data file, via automated gating and labeling, emerges as an important innovative step in standardization and simplification of flow cytometry data analysis.

Here we describe the steps required to build EuroFlow reference data bases for automated gating and classification of individual events contained in flow cytometric data files using peripheral blood (PB) samples stained with the EuroFlow Lymphoid Screening Tube (LST) panel as illustrating model. Data base construction steps consisted of: i) staining and selection of samples to be included in the data base; ii) evaluation of the data files corresponding to the reference samples selected and; iii) validation of the data base against independent sets of flow cytometry data files from both normal and pathological samples, stained and measured using identical procedures and antibody panels.

2. Material and methods

2.1. Samples

A total of 211 PB samples stained with LST and measured at 5 different EuroFlow laboratories between 2009 and 2018, were included in this study. Of these 211 samples, 129 were obtained from healthy donors (HD) and 82 were from patients diagnosed with chronic lymphoproliferative disorders (CLPD): B-cell CLPD (B-CLPD), 51 samples (40 chronic lymphocytic leukemias cases, three follicular lymphomas, two hairy cell leukemias, five mantle cell lymphomas and one splenic marginal zone lymphoma); and T/NK-cell CLPD (T/NK-CLPD), 31 samples (one adult T-cell leukemia/lymphoma, four Sézary syndromes, two T-cell prolymphocytic leukemias, 20 T-cell large granular lymphocyte leukemias, and four NK-cell chronic lymphoproliferative disorders). One hundred and nineteen of these PB samples were used to build the data base (set of test samples), while 92 were used as a validation set, consisting of PB samples from 10 HD/reactive conditions and 82 CLPD patients. The latter 92 samples in the validation set, were randomly selected from the pool of fully characterized and quality-controlled samples collected for validation of the EuroFlow data base. Quality control used for these samples included: fully annotated WHO diagnosis and both demographics and clinical and laboratory data; staining with the full LST antibody panel; and, exclusion of fluorescence compensation artifacts.

Reference values for the major leucocyte and lymphocyte (B-, T- and NK-cell) populations in PB, were defined based on 187 PB samples stained with the EuroFlow primary immunodeficiency orientation tube (PIDOT) as described elsewhere (van der Burg et al., 2019). Of note, LST and PIDOT share the most relevant markers to properly identify the major leukocyte and lymphocyte cell populations and provided identical results, as confirmed in a subset of 8 samples stained in parallel with both the PIDOT and the LST. These 187 individuals were divided into four age groups: i) < 15 years of age (y) (n = 122); ii) 15-30y (n = 25); iii) 31-50y (n = 20) and; > 50y (n = 20). In turn, reference values for surface membrane immunoglobulin (smIg) κ^+/smIgλ^+ ratio were taken from the literature (Szczepanski et al., 2006) and they have been confirmed in the 46 LST-stained normal/reactive PB samples.

In all cases, samples were collected after written informed consent had been given by each donor or their parents, according to the Declaration of Helsinki. Samples were then processed and stained locally at each center, using EuroFlow standard operating procedures (SOPs) for sample preparation and staining, and data acquisition (Kalina et al., 2012) available at www.EuroFlow.org. Samples stained with LST and/or PIDOT were measured in FACSCanto II -Becton Dickinson Biosciences (BD), San Jose, CA- flow cytometers, calibrated and monitored according to the EuroFlow SOP for instrument set-up (Kalina et al., 2012), also available at www.EuroFlow.org.

The study was approved by the local ethics committees of the participating centers.

2.2. Construction of the normal reference data base

To construct the reference LST data base of normal/reactive PB samples (LST-PB data base), datafiles corresponding to 119 HD/reactive PB samples stained with the EuroFlow LST antibody panel, were used. After data acquisition, and prior to data analysis, the technical quality of each data file was evaluated. This included the following assessments: i) confirmation of inclusion of data about all informative parameters in each data file -e.g. forward scatter height (FSC-H) in addition to standard scatter and fluorescence parameters-; ii) appropriate compensation profiles, as described elsewhere (Kalina et al., 2012; Tung et al., 2004); iii) expected intensity of staining for each marker (or group of markers) per fluorochrome in pre-defined control cell populations (Supplemental Table 1); and, iv) identification of outliers (> 1.5 times interquartile ranges). All data files failing to meet one or more of the above pre-established criteria, including outliers, were excluded from the data base and from further processing (Fig. 1).

2.3. Data base validation

The validation data file set consisted of data files derived from flow cytometry measurements of normal/reactive and CLPD PB samples stained with the EuroFlow LST panel. Each normal/reactive and CLPD data file was analyzed using the Infinicyt software (version 2.0; Cytognos SL, Salamanca, Spain). Data analysis included the following

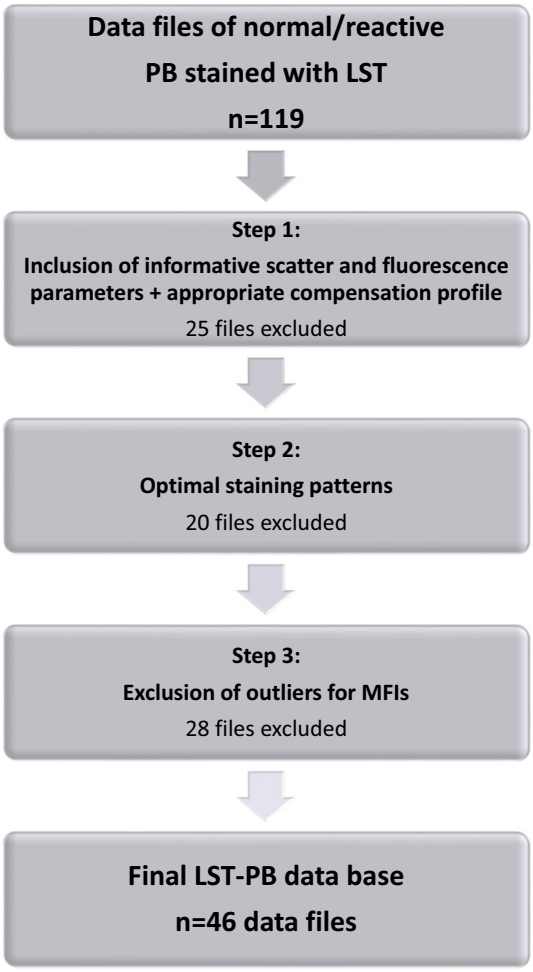

Fig. 1. Schematic representation of sequential steps followed to select PB samples (n = 46/119) to be included in the LST-PB reference data base.

steps: i) automated gating based on unsupervised clustering algorithms where ≥10 events were required per cluster (i.e. K parameter) at a maximum distance/dispersion within the cluster of 0.9 (i.e. S parameter), as previously described in detail (Fluxá Rodriguez et al., 2017); ii) quantitative comparison of the expression profile of the different immunophenotypic characteristics of each cluster of events obtained in the previous step against every cell population in the reference data base using multiparameter analysis -i.e., principal component analysis (PCA)(Jolliffe, 2002) and canonical clustering analysis (CA)(Fujikoshi et al., 2010)-; iii) classification (i.e. labelling) of those clusters of events, as phenotypically identical or not to a cell population. Thus, clusters of events that fully matched (i.e. fall within 2.5 SD) the phenotypic features of a given (single) cell population in the reference data base were classified as corresponding to that specific cell population. In contrast, other clusters of events showing differences (either phenotypic differences or numerical differences) versus the distinct cell populations in the reference data base, were automatically "alarmed" as populations to be checked by an expert (i.e. alarmed cluster of events/cell populations).

2.4. Statistical methods

The Kolmogorov-Smirnov test was used to assess data distribution. Outliers were identified as those values below or above 1.5 times the interquartile range values (i.e. < 1st quartile or > 3rd quartile) for individual scatter and fluorescence parameters. Statistical significance of differences between two or more independent groups was evaluated using the Mann-Whitney U or the Kruskal-Wallis tests, respectively. For correlation studies, the Pearson's correlation analysis or the Spearman's *rho* tests were used for normal and non-normal data distribution, respectively. Statistical significance was set at values ≤.05. For all statistical analyses the Statistical Package for Social Sciences (SPSS) software (version 23; IBM, Armonk, NY) was used.

3. Results

3.1. Selection of flow cytometry data files from normal/reactive PB samples to be included in the LST-PB data base

To build the LST-PB reference database, flow cytometric data files from 119 normal/reactive PB samples stained with the EuroFlow LST panel, were used. Each of these data files was independently analyzed by two experts following pre-defined sequential manual gating steps, as illustrated in Fig. 2. Briefly, a sequence of ("Boolean") gates was first used to identify each cell population in individual LST-stained normal/reactive PB samples, using a combination of their light scatter properties and/or immunophenotypic profile (Table 1 and Fig. 2A_1 and A_2). Then, debris and cell doublets -i.e. events with lower forward scatter and/or placed outside the forward scatter (FSC)-Area vs FSC-Height plot diagonal- (Fig. 2B_1 and B_2), were excluded from all previously gated cell populations. Subsequently, the major lymphocyte (sub)sets (e.g. smIgκ$^+$ and smIgλ$^+$ B-cells and CD4$^+$, CD8$^+$, TCRγδ$^+$ and CD4$^-$/CD8$^-$/TCRγδ$^-$ T cell populations) in addition to NK-cells, monocytes, neutrophils and eosinophils were identified, and remaining cells showing unspecific stainings excluded from each gated leucocyte population (Fig. 2C_1 and C_2). Finally, each cell population identified was assigned to its corresponding position in a pre-defined (hierarchical) population tree. Clusters of events displaying leukocyte-matching light scatter properties, (after exclusion of debris and cell doublets) and positive staining for ≥1 LST marker (e.g. CD45), but that could not be clearly categorized as a unique specific cell population (e.g. dendritic cells and basophils), were labeled as "Unspecified nucleated cells" in the population tree.

3.2. Quality assessment of normal/reactive PB flow cytometric data files to be included in the LST-PB data base

After all flow cytometric data files corresponding to LST-stained normal/reactive PB samples (n = 119) had been manually analyzed, their technical quality was individually assessed (Fig. 1). Thus, 25 data files without stored FSC-H data, that showed inappropriate fluorescence compensation and/or displayed other technical issues, were excluded from further data base construction steps. The remaining 94 data files were checked for appropriate staining patterns. For this purpose, file number vs individual parameter dot plots were used to: i) confirm all (relevant) cell populations were present in every data file, and ii) directly compare their staining profiles for every individual marker. Twenty additional data files were further excluded at this stage. Subsequently, outlier data files (n = 28), defined as those displaying median fluorescence/scatter intensity (MFI) values lower or higher than the 1.5 interquartile range for the corresponding positive reference cell population (PRCP) and negative reference cell population (NRCP) (Supplemental Table 1) were also excluded from the LST-PB data base at this step (Fig. 1). The remaining 46 data files were merged and included in the reference LST-PB data base. Finally, every cell population from each PB sample was compared against the corresponding cell populations in all other data files using CA, to confirm that the phenotypic profile of every cell population in each individual data file was within 2.5 SD of the paired cell populations in the other 45 files in the data base (Fig. 3).

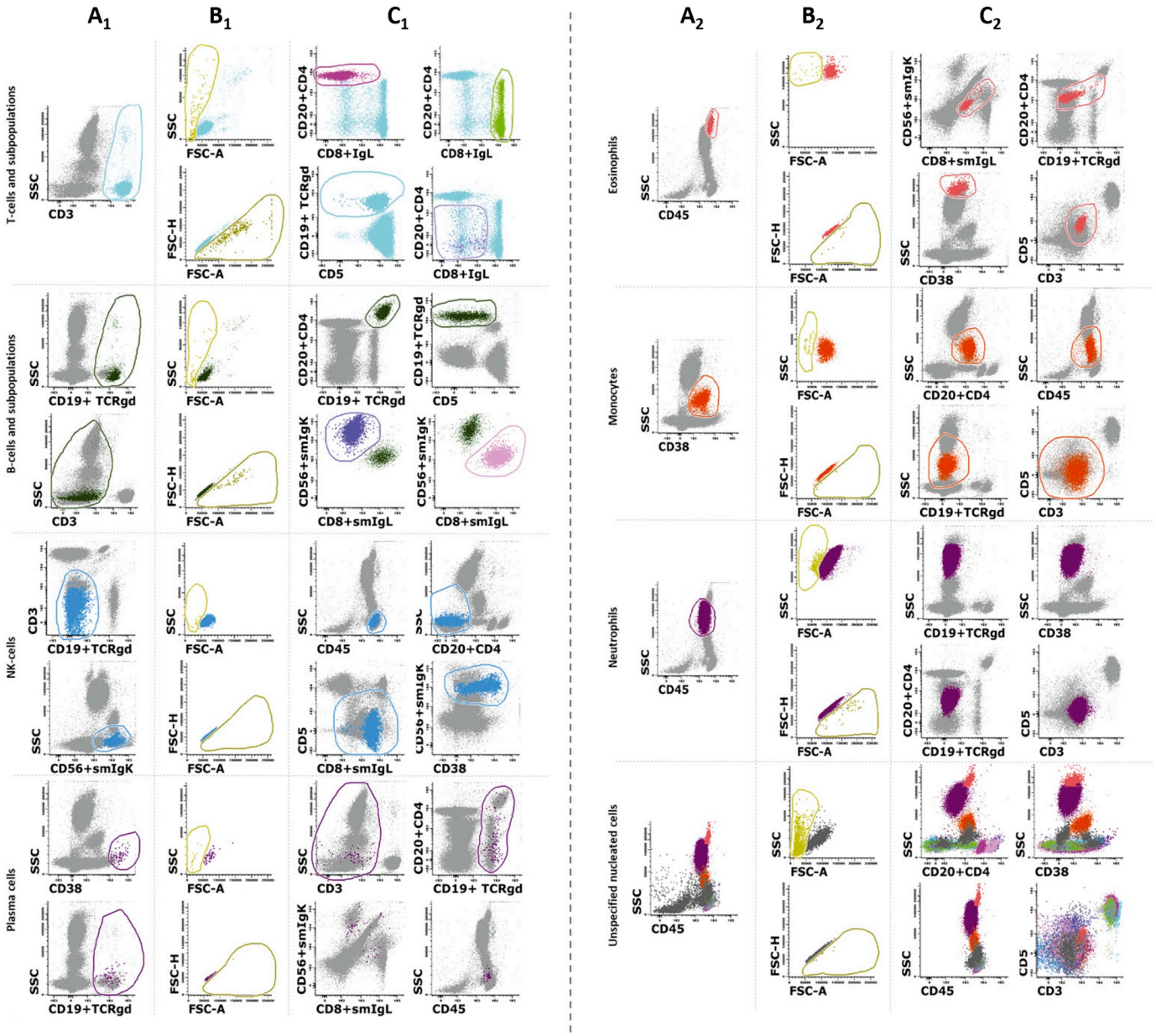

Fig. 2. LST-PB data base construction: illustrating example of the Boolean gating strategy used to identify distinct populations of nucleated cells present in normal human PB stained with LST. All different major cell populations present in the data files of normal/reactive PB samples selected to build the LST-PB data base -i.e. T- (light blue dots), B- (dark green dots) and NK-cells (blue events) and, plasma cells (violet dots), eosinophils (pink dots), monocytes (orange events) and neutrophils (dark violet events), as well as "unspecified nucleated cells" (dark grey events)- (panels A_1 and A_2) were first identified based on their distinct light scatter properties and phenotypic profile. Subsequently, (panels B_1 and B_2) debris (i.e. light yellow/green events with lower FSC-A) and cell doublets (i.e. dark yellow/green events out of the diagonal in the FSC-H vs FSC-A dot plots) were excluded from each of the gates drawn in panels A_1 and A_2. Then, T- and B-cells were further subclassified as $CD4^+/CD8^-$ (pink events), $CD8^+/CD4^-$ (light green dots), $TCR\gamma\delta^+$ (light blue dots) and $CD4^-/CD8^-/TCR\gamma\delta^-$ (violet dots) and as surface membrane (sm) $Ig\kappa^+$ (light violet dots) and $smIg\lambda^+$ (light pink dots), respectively (panels C_1 and C_2). For all cell populations, events showing unspecific staining profiles were further identified and excluded from each population. Further information about the phenotypic profile of each cell population in the LST-PB data base is shown in Table 1. (For interpretation of the references to color in this figure legend, the reader is referred to the web version of this article.)

3.3. Normal/reactive PB reference count values per age group

Multivariate analysis of the phenotypic characteristics of the distinct normal PB cell populations identified according to age (i.e. < 15y; 15-30y, 31-49y and ≥ 50y) showed highly similar and overlapping patterns of antigen expression (data not shown). However, distinct age-group associated cell counts were observed among the 187 normal PB samples stained with PIDOT (Table 2). Thus, < 15y controls showed significantly ($p \leq .05$) higher lymphocyte (relative) counts than older subjects (Table 2). In contrast, healthy children < 15y showed lower neutrophil (relative) counts than healthy adults > 15 years (Table 2). Comparison of the relative cell counts with LST vs PIDOT performed in a subset of 8 normal PB samples stained in parallel with both antibody combinations showed no significant differences for any cell population identified ($p < .05$) with a very high degree of correlation among them ($r^2 = 0.99$; $p < .001$). Reference values used for $smIg\kappa^+/smIg\lambda^+$ ratio were taken from the literature (median 1.4%, range: 0.8%–2.4%) (Szczepanski et al., 2006) and they were further confirmed in the 46 LST-stained normal/reactive PB samples included in the reference LST-PB data base (median 1.4%, range: 1%–2%).

Table 1
Distinct cell populations identified in normal/reactive reference PB samples with LST.

Cell population	Main phenotypic features
Mature B-cells	SSC^{lo}, FSC^{lo}, $CD45^+$, $CD19^+$, $CD20^+$, $CD3^-$
smIgκ	$smIg\kappa^+$, $smIg\lambda^-$
smIgλ	$smIg\lambda^+$, $smIg\kappa^-$
T-cells	SSC^{lo}, FSC^{lo}, $CD45^+$, $CD3^+$, $CD19^-$
CD4	$CD4^+$, $CD8^-$
CD8	$CD8^+$, $CD4^-$
TCRγδ	$CD4^-$, $CD8^-$, $TCR\gamma\delta^+$
$TCR\gamma\delta^-$ ($CD4^-$, $CD8^-$)	$CD4^-$, $CD8^-$, $TCR\gamma\delta^-$
NK cells	SSC^{lo}, FSC^{lo}, $CD45^+$, $CD19^-$, $CD20^-$, $CD3^-$, $CD56^{lo/+}$
Circulating plasma cells	SSC^{int}, FSC^{int}, $CD38^{hi}$, $CD45^{-/lo}$, $CD19^+$
Eosinophils	SSC^{hi}, FSC^{Int}, $CD45^{hi}$, other markers$^-$ (autofluorescent in some channels)
Neutrophils	$SSC^{int/hi}$, $FSC^{int/hi}$, $CD45^+$, other markers$^-$
Monocyte	SSC^{int}, FSC^{int}, $CD45^+$, $CD4^+$, $CD38^+$
Unspecified nucleated cells	Light scatter properties compatible with leukocytes and ≥ 1 positive marker in the combination, but not categorized as unique distinct cell population[a]

SSC, sideward light scatter; FSC, forward light scatter; sm, surface membrane; Ig, immunoglobulin; TCR, T cell receptor; lo, low; int, intermediate; hi, high.
[a] Includes basophils and/or dendritic cells for which no LST markers exist for their positive identification.

3.4. Validation of the EuroFlow LST-PB reference data base

To validate the LST-PB reference data base, 92 data files from 10 HD and 82 CLPD patients were used. For this purpose, each FCS data file from the validation set was compared with the reference data base, using the automated gating and classification algorithms described above in the Material and methods section of this manuscript using Infinicyt software. This included two sequential steps: i) clustering of individual events; and, ii) classification of clusters of events into cell populations.

In the clustering step, a mean of 336 (± 267) clusters (i.e. groups of events with similar characteristics in the multidimensional space generated by all parameters evaluated) were identified, using a minimum number of 10 events/cluster (K) with a maximum dispersion/distance (S) of 0.9. In the classification step, all individual clusters of events obtained per data file, were compared with each pre-defined cell population in the reference LST-PB data base for both their phenotypic profile -PCA and CA- and relative distribution according to age. In normal/reactive samples from the validation set ($n = 10$), the vast majority of events in the data file -median of 99.2% (range 95.5%–99.7%)- were correctly classified into one of the normal cell populations in the data base; in contrast, in the abnormal/pathological samples, while the majority -median of 55.6% (range 1%–98.7%)- of events were classified as belonging to the distinct normal cell populations in the reference data base, a large fraction of them -median of 44.4% (range: 1.3%–99%)- were alarmed, and required to be checked by an expert due to phenotypic deviations (62/82; 75.6%) and/or numeric alterations (71/82; 86.6%), for 82/82 (100%) alarmed CLPD cases. Thus, 18/82 (22%) data files were alarmed based on an altered relative distribution of ≥1 cell population, while 72/82 data files (78%) had both phenotypic and numerical alarms for tumor cells. Of note, a correlation ($rho = 0.76$, $p < .001$) was observed between the percentage of events alarmed (to be checked) and the actual percentage of abnormal cells present in the sample, as identified by expert-based (manual) analysis -median of 49.8% (range: 1.3%–96.2%)-. As expected, automated gating typically tagged the abnormal CLPD population as “check” under a specific lymphoid cell population (i.e. B-, T- or NK-cells) according to its specific phenotypic profile. Interestingly, cases that only showed numerical alarms (18/82, 22%) systematically corresponded to T/NK CLPD (18/18; 100%). In 15/82; (18.3%) samples, technical alarms were also found, as reflected by an increased number of checks (≥5% higher than the percentage of abnormal cells as identified by the experts). Finally, in 2/82 (2.4%) samples two abnormal populations were simultaneously detected, both being correctly alarmed during automated gating. The alarmed clusters of events were assigned either to a normal or abnormal cell population by two independent experts with a high degree of agreement on the type and number of normal/residual as well as clonal/aberrant cells among them (data not shown). Similarly, an overall high degree of correlation between the type and number of normal -largely represented (i.e. > 5%) and less abundant (i.e. ≤5%)- cell populations and abnormal CLPD cell populations was found between the proposed automated method and conventional expert-based manual classification approaches ($r^2 = 0.96$, $p < .001$; $r^2 = 0.84$, $p < .001$ and $rho = 0.99$, $p < .001$, respectively) (Fig. 4).

4. Discussion

Due to recent technical developments, data analysis in multiparameter flow cytometry has become increasingly complex and time consuming. This has challenged the capability of flow cytometry experts to perform cost-effective analysis and interpretation of data files containing information about progressively higher numbers of events, markers and cell populations (Mair and Prlic, 2018; Perfetto et al., 2004; Staser et al., 2018). Current expert-based conventional strategies for processing and interpreting flow cytometry data are strongly dependent on individual expertise and prone to subjectivity. With the increase of the complexity and volume of flow cytometry data, experts have adopted different strategies based on e.g. predefined (gating) templates for analysis or preferential focus on one (or a few) cell populations per sample, thereby ignoring the potential relevance of other cell populations. Some centers have chosen restricted antibody panels, only identifying major cell populations, such as total T-, B- and, NK cells in patients suspicious of primary immunodeficiency. The corresponding manual analysis strategies used in individual laboratories or by individual experts are hardly reproducible, because minor deviations in subsequent gating steps and/or the markers selected to identify a cell population will easily generate different results (Finak et al., 2016). This diversity in strategies emphasizes the need for simpler, less laborious, less time-consuming, and more reproducible gating strategies.

Automation of cell identification allows robust and reproducible gating and has emerged as an attractive approach to overcome the limitations of manual expert-based gating (Bandura et al., 2009; Futamura et al., 2015; Lugli et al., 2010; Pedreira et al., 2019, 2008a, 2013; Perfetto et al., 2004). However, in virtually all automated gating approaches described so far, the expert's input is still required, for example, to assign groups of events to specific cell populations producing highly variable results (Chester and Maecker, 2015; Kalina et al., 2012; Meehan et al., 2014; O'Neill et al., 2013; Pedreira et al., 2013, 2008b; Petrausch et al., 2006; Saeys et al., 2016). In order to overcome this limitation, the EuroFlow consortium has designed, constructed and validated an automated gating and classification strategy based on combined use of i) clustering techniques to define groups of events in a sample; and, ii) a data base comparison step, to (objectively) classify each individual group of events in a sample against pre-defined cell populations in a data base (matched for sample type, antibody panel, age and/or disease condition)(Pedreira et al., 2019), as exemplified here for the LST in normal vs CLPD samples.

Generation of standardized and high-quality data is a pre-requisite for successful automation of gating of (all) cell populations coexisting in a data file, as recently recognized and addressed by the EuroFlow Consortium (Flores-Montero et al., 2017; Kalina et al., 2012; Lhermitte et al., 2018; Nováková et al., 2017; Theunissen et al., 2016; van der Burg et al., 2019; van Dongen et al., 2012). Successful automation of data analysis in clinical flow cytometry requires the use of standardized antibody panels, instrument calibration, and sample preparation, to assure that data files from different samples, measured on different

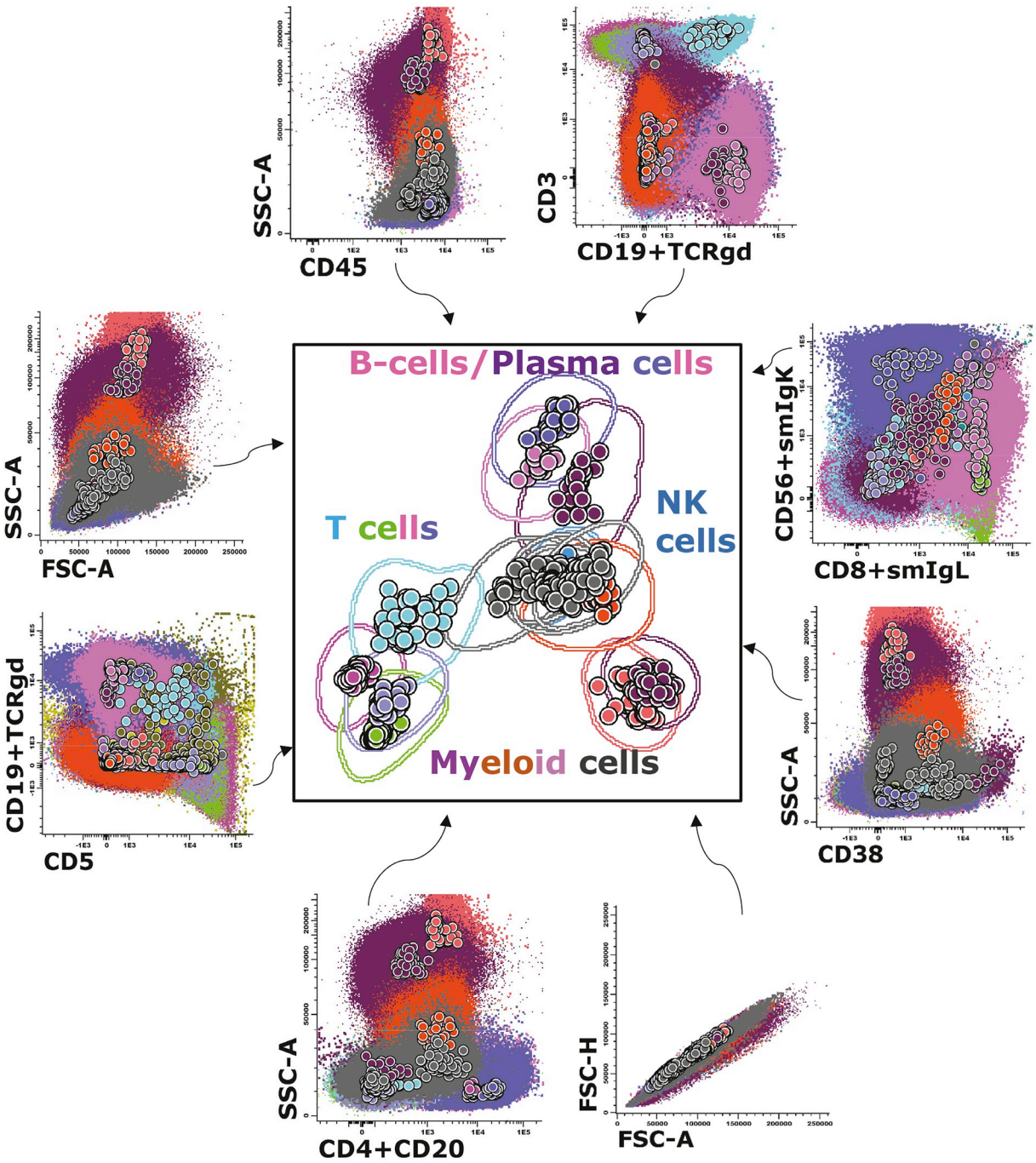

Fig. 3. Schematic representation of merged reference data files included in the LST-PB data base. Peripheral plots are classic bivariate representations of the 46 high quality data files of LST-stained normal/reactive samples merged into the reference LST-PB data base using Infinicyt software. In turn, the central plot shows a bidimensional summary plot of all parameters evaluated using a multivariate data analysis graphical representation -i.e. canonical analysis (CA)- available in the Infinicyt software. Peripheral plots highlight overlapping phenotypic profiles observed for the same cell populations identified in each individual data file. Different cell populations are color coded and represented both as colored events and their median values (colored larger circles) for all parameters displayed in each (peripheral) conventional bidimensional dot plots. In turn, in the CA plot in the middle panel, median values for all parameters in the data file (colored circles) and the corresponding 2.5 SD (empty lines) for each cell population in the data base, are shown in the CA multivariate analysis graphical representation. Every color represents a different cell population of lymphoid and myeloid cells as color coded in the text inside the central plot.

days, with different flow cytometers, by different technicians, will contain highly comparable (i.e. identical) data. In addition, such standardized panels should be appropriate for identification of all potential (normal and aberrant) cell populations in the investigated samples.

Here we used the EuroFlow LST antibody panel (van Dongen et al., 2012) in combination with the EuroFlow instrument calibration and sample preparation SOPs (Kalina et al., 2012) to build and validate the EuroFlow LST-PB data base (Pedreira et al., 2019). To build the data base, highly strict criteria were used for inclusion of data files in order to avoid variability caused by identifiable and recognizable technical artifacts that have a negative impact on the overall performance of this strategy. Because of this strict selection, only a fraction (≈40%) of all data files met the required criteria for inclusion into the data base. This strict selection appeared to be key to assure an accurate automated

Table 2
Distribution of different cell populations in normal/reactive PB samples (n = 187) used to define relative distribution reference values according to age.

Cell population	Age groups				All ages
	< 15y	15-30y	31-49y	≥50y	
	n = 122	n = 25	n = 20	n = 20	n = 187
Lymphocytes	43.6% (23.3%–72.5%)	28.8%[a] (15.8%–47.5%)	32.9%[a] (14.5%–43.9%)	37.7%[a,b,c] (27.4%–47.8%)	39.3% (19.6%–69.1%)
T cells	32.1% (14.9%–53.3%)	20.8%[a] (12.5%–35.7%)	23.1%[a] (10.2%–34.7%)	30.6%[b,c] (17.7%–40.4%)	29.8% (14.5%–50.4%)
$CD4^+CD8^-$	20.1% (9.6%–37.3%)	13.6%[a] (7.2%–24%)	14.2%[a] (6.6%–21.9%)	17.0%[b,c] (10.4%–25.6%)	17.0% (8.7%–33.2%)
$CD8^+CD4^-$	9.1% (3.8%–17.7%)	6.6%[a] (3.6%–14.1%)	7.3%[a] (2.3%–17.3%)	9.4%[a,b] (2.9%–19.8%)	8.5% (3.5%–17.7%)
$TCR\gamma\delta^+$	2.1% (0.3%–5.5%)	1.0%[a] (0.2%-3.5)	0.8%[a] (0.2%–3.2%)	1.0%[a,b] (0.1%–2.7%)	1.6% (0.3%–4.5%)
$CD4^-/CD8^-/TCR\gamma\delta^-$	0.3% (0.1–0.9%)	0.2%[a] (0.08%–0.6%)	0.2%[a,b] (0.06%–0.4%)	0.1%[a,b] (0.03%–0.3%)	0.3% (0.07%–0.8%)
CD4/CD8 ratio	2.2 (0.9–4.5)	1.8[a] (1–3.6)	1.8 (0.9–3.8)	1.8[c] (0.5–6.4)	2.0 (0.5–6.4)
Mature B cells	7.2% (2.8%–15%)	3.5%[a] (1%–5.6%)	2.6%[a] (0.7%–5.7%)	2.6%[a] (1%–4.6%)	5.1% (1.4%–14.5%)
NK cells	4.7% (2%–10.8%)	3.3%[a] (1.4%–8.6%)	5.0%[b] (2.3%–10.8%)	5.0%[b] (1.9%–8.7%)	4.7% (2%–9.9%)
Plasma cells	0.2% (0.03%–0.5%)	0.05%[a] (0.02%-0.1%)	0.04%[a,b] (0.01%–0.08%)	0.02%[a,b,c] (0.01%–0.05%)	0.07% (0.01%–0.4%)
Eosinophils	2.3% (0.4%–5.6%)	1.6%[a] (0.4%–3.2%)	2.1%[a,b] (0.4%–20.6%)	1.5%[a] (0.03%–4.3%)	2.1% (0.4%–5.6%)
Neutrophils	42.1% (15%–66%)	58.2%[a] (40.5%–75.5%)	55.4%[a,b] (34.8%–73.7%)	50.6%[a,b] (37.9%–60.5%)	46.6% (18.4%–67.7%)
Monocytes	8.3% (4.5%–13%)	8.0% (3.7%–11.2%)	8.7% (5%–16.6%)	8.8% (5.7%–12.9%)	8.4% (4.7%–13%)

Results expressed as median % (5%–95% reference ranges) values. All percentages are referred to nucleated cells, after excluding debris and cell doublets.
[a] $p < .05$ vs < 15y age group.
[b] $p < .05$ vs 15-30y age group.
[c] $p < .05$ vs 31-49y age group.

classification of cell populations via the data base. In fact, validation of the LST-PB data base in conjunction with the automated gating and classification procedure showed very few alarms (typically event rates of < 1%) in normal/reactive samples. In contrast, events rates of ≈40% were associated with alarms in data files from CLPD involved specimens. In addition to minor alarms found for a few normal cell populations, major alarms were detected for the bulk of CLPD populations. This translated into a sensitivity of 100% with also a high specificity (99%) for alarms ≥5% of total tumor CLPD cells. Interestingly, in 2 cases, two different abnormal cell populations were simultaneously identified because they were separately alarmed in the same data file, allowing diagnosis of CLPD patients with more than one tumor cell population. This is due to the fact that automated analysis is not specifically focused on one or a few cell populations in the sample, but considers all cell populations present, thereby contributing to sensitive identification of samples containing ≥2 distinct (related or unrelated) tumor cell populations. Thus, in the proposed automated classification approach, iterative comparison of each cluster vs the reference population is performed. Consequently, the presence of clusters of events which do not match any normal reference cell population, is automatically highlighted (i.e. alarmed), even if these cell populations are not directly related to the actual reason for sample evaluation. In fact, this automated cell classification checks for normal vs altered phenotypes and/or normal vs altered cell numbers for any cell population in individual data files, avoiding overlooking any abnormal cell population, as might occur during expert-based manual analysis.

A key feature of the EuroFlow automated gating strategy used here, relies on how reference data bases of normal cell populations are built and on its representativeness for the biological variability that can be observed in large sets of normal PB samples, e.g. age-related distribution of cell populations. As discussed above, technical variability should be minimized via standardization of all procedures involved, in such a way that the main source of differences reflects biologic variability or actual cell alterations due to aberrant phenotypic profiles and/or altered cell numbers vs age-matched controls. Of note, here we confirm that the patterns of antigen expression of normal/reactive cell populations are highly consistent in line with previous observations (Flores-Montero et al., 2017; Szczepanski et al., 2006; van Dongen et al., 2012). Thus, normal biologic variability is typically well represented even with relatively limited numbers of normal samples. In contrast, even among homogeneous cohorts of PB samples from healthy donors, leukocyte and lymphocytes counts vary significantly with age, as previously shown by our and other groups (Blanco et al., 2018; Comans-Bitter et al., 1997; Damasceno et al., 2019; Lucio et al., 1999; Shearer et al., 2003; van Dongen et al., 2019; van Lochem et al., 2004), and confirmed here also for the cell populations identified in PB with the LST tube. Consequently, in order to increase the sensitivity of LST to detect abnormal cell populations, the use of numerical alarms requires prior definition of normal age-related reference ranges. Thus, for the LST-PB, four distinct age-associated categories of "normal PB samples" were deemed. Of note, although absolute count values were not considered here, they might also be used to alarm for counts that are lower or higher than normal values for each PB cell population identified with LST. However, regardless of the differences in antibody composition between the PIDOT and LST tubes, both share a main set of markers devote to identify the relevant leukocyte and lymphocyte cell populations in PB, providing identical counts for e.g. the major T-, B-, and NK-cell populations as confirmed here via parallel staining of a group of samples with both PIDOT and LST. Altogether, these results support the use of age associated reference values for these cell populations as obtained with PIDOT, also for LST. In addition, reference values from smIgκ/smIgλ ratio were taken from the literature (Szczepanski et al., 2006) and confirmed in the 46 normal/reactive PB samples stained with the LST. Collection of a

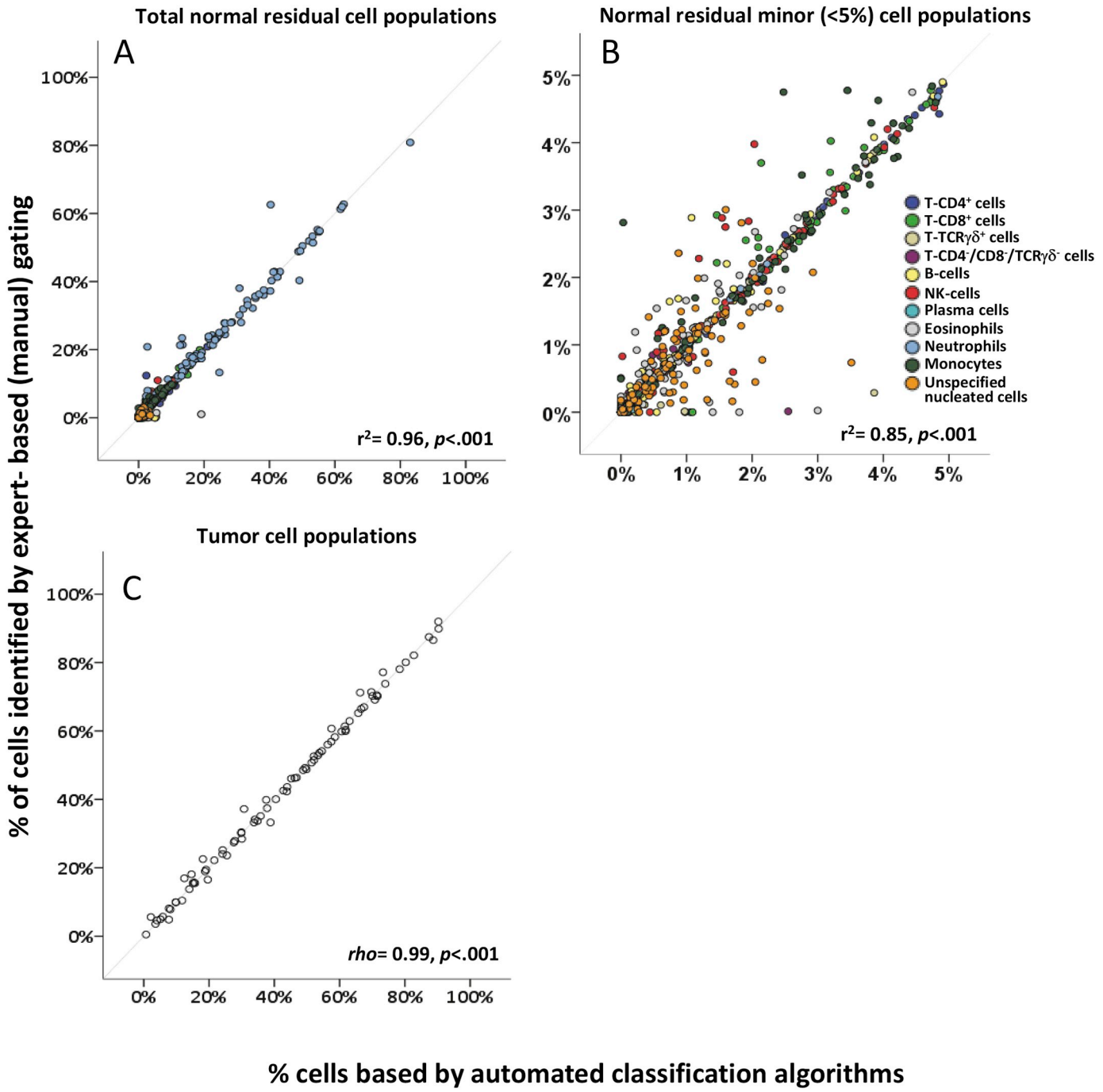

Fig. 4. Correlation between the number of total normal residual cells (panel A), including those normal residual cells present at frequencies below 5% (panel B), and tumor cells (panel C) in PB samples from both healthy donors (n = 10) and CLPD patients (n = 82) evaluated either using automated gating with the LST-PB data base or conventional expert-based manual gating.

higher number of controls to define age-associated reference ranges with the LST-PB is ongoing.

Thus, validation of the data base against a large set of normal and CLPD data files showed that the new EuroFlow automated gating approach can satisfactorily replace manual gating strategies in routine laboratory diagnostics. Of note, direct prospective comparison of data from newly obtained data files, against the (normal) LST-PB data base also highlighted (minor) technical problems occurring in a small subset of PB data files from the validation set as reflected by a higher rate (> 5%) of normal/residual cells being alarmed. Such increased alarm rates were due to a larger technical variability, reduced overall sample quality, and/or an impact of the underlaying disease on the distribution of the other residual cell populations (data not shown). Thus, this < 5% threshold of alarms for normal cells might be used as a criterion to identify successful performance of the whole strategy. In such cases, the data base acts as an "in sample" external quality check through which staining profiles obtained in a sample are directly compared with an "external" data base of reference "normal" properly-stained samples, providing an innovative tool to assess also the quality of data.

A major obstacle in standardization concerns variations in both analytical and pre-analytical steps. Among other factors, reproducibility of the results strongly depends on the quality of the sample, influenced by anticoagulant, transport time and temperature during transportation, time and temperature prior to staining and the flow

cytometry measurement, quality of reagents between different lots from one manufacturer, and between reagents from different manufacturers, reagent deterioration over time, inappropriate reagent handling and storage conditions (Böttcher et al., 2017; O'Donnell et al., 2013). Usage of the EuroFlow data bases also requires standardization of all pre-analytical steps, as recently shown by Diks et al. (2019). Strict standardization and control of (all) steps involved in flow cytometric phenotyping, prior to data analysis, will also contribute to more reproducible and higher quality results. The here described strategy for data analysis, based on data base-guided automated gating provides the basis for a real-time external quality control of all individual samples analyzed against (multicenter) reference data bases.

In summary, our results show that automated identification of cell populations based on the EuroFlow LST-PB data base available via the Infinicyt software provides an innovative, reliable and reproducible tool for the recognition of normal and pathological B and T/NK lymphocytes in PB in patients with CLPD, with a great contribution potential for standardization of clinical flow cytometry assays within as well as outside the EuroFlow laboratories.

Supplementary data to this article can be found online at https://doi.org/10.1016/j.jim.2019.112662.

Acknowledgements

This work was supported by the CB16/12/00400 and CB16/12/00369 grants, CIBER-ONC, Instituto de Salud Carlos III, Ministerio de Economía y Competitividad, Madrid, Spain and FONDOS FEDER; DTS 15/00119 grant, Instituto de Salud Carlos III, Ministerio de Economía y Competitividad, Madrid, Spain and FONDOS FEDER; and, RETOS (RTC–2016–4865–1) grant, Sociedad de la Acción Estratégica de Economía y Sociedad Digital-Impulso Tecnológico; Ministerio de Economía y Competitividad, Madrid, Spain.

References

Bandura, D.R., Baranov, V.I., Ornatsky, O.I., Antonov, A., Kinach, R., Lou, X., Pavlov, S., Vorobiev, S., Dick, J.E., Tanner, S.D., 2009. Mass cytometry: technique for real time single cell multitarget immunoassay based on inductively coupled plasma time-of-flight mass spectrometry. Anal. Chem. 81, 6813–6822. https://doi.org/10.1021/ac901049w.

Blanco, E., Pérez-Andrés, M., Arriba-Méndez, S., Contreras-Sanfeliciano, T., Criado, I., Pelak, O., Serra-Caetano, A., Romero, A., Puig, N., Remesal, A., Torres Canizales, J., López-Granados, E., Kalina, T., Sousa, A.E., van Zelm, M., van der Burg, M., van Dongen, J.J.M., Orfao, A., 2018. Age-associated distribution of normal B-cell and plasma cell subsets in peripheral blood. J. Allergy Clin. Immunol. 141, 2208–2219.e16. https://doi.org/10.1016/j.jaci.2018.02.017.

Blanco, E., Pérez-Andrés, M., Arriba-Méndez, S., Serrano, C., Criado, I., Del Pino-Molina, L., Silva, S., Madruga, I., Bakardjieva, M., Martins, C., Caetano, A.S., Romero, A., Contreras-Sanfeliciano, T., Bonroy, C., Sala, F., Martín, A., Bastida, J.M., Lorente, F., Prieto, C., Dávila, I., Marcos, M., Kalina, T., Vlkova, M., Chevankova, Z., Cordeiro, A.I., Philippé, J., Haerynck, F., López-Granados, E., da Sousa, A.E., van der Burg, M., van Dongen, J.J.M., Orfao, A., 2019. Defects in memory B-cell and plasma cell subsets expressing different immunoglobulin-subclasses in CVID and Ig-subclass deficiencies. J. Allergy Clin. Immunol. https://doi.org/10.1016/j.jaci.2019.02.017.

Böttcher, S., van der Velden, V.H.J., Villamor, N., Ritgen, M., Flores-Montero, J., Murua Escobar, H., Kalina, T., Brüggemann, M., Grigore, G., Martin-Ayuso, M., Lecrevisse, Q., Pedreira, C.E., van Dongen, J.J.M., Orfao, A., 2017. Lot-to-lot stability of antibody reagents for flow cytometry. J. Immunol. Methods. https://doi.org/10.1016/j.jim.2017.03.018.

Chattopadhyay, P.K., Lomas III, W.E., Laino, A.S., Winters, A.F., Woods, D.M., 2019. High-parameter single-cell analysis. Annu. Rev. Anal. Chem. 12https://doi.org/10.1146/annurev-anchem-061417-125927. annurev-anchem-061417-125927.

Chester, C., Maecker, H.T., 2015. High-dimensional cytometry data algorithmic tools for mining algorithmic tools for mining high-dimensional cytometry data. J. Immunol. 195, 773–779. https://doi.org/10.4049/jimmunol.1500633. Mater. Suppl. plemental.html.

Comans-Bitter, W.M., de Groot, R., van den Beemd, R., Neijens, H.J., Hop, W.C., Groeneveld, K., Hooijkaas, H., van Dongen, J.J., 1997. Immunophenotyping of blood lymphocytes in childhood. Reference values for lymphocyte subpopulations. J. Pediatr. 130, 388–393. https://doi.org/10.1016/s0022-3476(97)70200-2.

Damasceno, D., Teodosio, C., van den Bossche, W.B.L., Perez-Andres, M., Arriba-Méndez, S., Muñoz-Bellvis, L., Romero, A., Blanco, J.F., Remesal, A., Puig, N., Matarraz, S., Vicente-Villardón, J.L., van Dongen, J.J.M., Almeida, J., Orfao, A., 2019. Distribution of subsets of blood monocytic cells throughout life. J. Allergy Clin. Immunol. https://doi.org/10.1016/j.jaci.2019.02.030.

Diks, A.M., Bonroy, C., Teodosio, C., Groenland, R.J., de Mooij, B., de Maertelaere, E., Neirynck, J., Philippé, J., Orfao, A., van Dongen, J.J.M., Berkowska, M.A., 2019. Impact of blood storage and sample handling on quality of high dimensional flow cytometric data in multicenter clinical research. J. Immunol. Methods. https://doi.org/10.1016/j.jim.2019.06.007.

Engel, P., Boumsell, L., Balderas, R., Bensussan, A., Gattei, V., Horejsi, V., Jin, B.Q., Malavasi, F., Mortari, F., Schwartz-Albiez, R., Stockinger, H., van Zelm, M.C., Zola, H., Clark, G., 2015. CD nomenclature 2015: human leukocyte differentiation antigen workshops as a driving force in immunology. J. Immunol. 195, 4555–4563. https://doi.org/10.4049/jimmunol.1502033.

Finak, G., Langweiler, M., Jaimes, M., Malek, M., Taghiyar, J., Korin, Y., Raddassi, K., Devine, L., Obermoser, G., Pekalski, M.L., Pontikos, N., Diaz, A., Heck, S., Villanova, F., Terrazzini, N., Kern, F., Qian, Y., Stanton, R., Wang, K., Brandes, A., Ramey, J., Aghaeepour, N., Mosmann, T., Scheuermann, R.H., Reed, E., Palucka, K., Pascual, V., Blomberg, B.B., Nestle, F., Nussenblatt, R.B., Brinkman, R.R., Gottardo, R., Maecker, H., McCoy, J.P., 2016. Standardizing flow cytometry immunophenotyping analysis from the human ImmunoPhenotyping consortium. Sci. Rep. 6. https://doi.org/10.1038/srep20686.

Flores-Montero, J., Sanoja-Flores, L., Paiva, B., Puig, N., García-Sánchez, O., Böttcher, S., van der Velden, V.H.J., Pérez-Morán, J.-J., Vidriales, M.-B., García-Sanz, R., Jimenez, C., González, M., Martínez-López, J., Corral-Mateos, A., Grigore, G.-E., Fluxá, R., Pontes, R., Caetano, J., Sedek, L., del Cañizo, M.-C., Bladé, J., Lahuerta, J.-J., Aguilar, C., Bárez, A., García-Mateo, A., Labrador, J., Leoz, P., Aguilera-Sanz, C., San-Miguel, J., Mateos, M.-V., Durie, B., van Dongen, J.J.M., Orfao, A., 2017. Next Generation Flow for highly sensitive and standardized detection of minimal residual disease in multiple myeloma. Leukemia 31, 2094–2103. https://doi.org/10.1038/leu.2017.29.

Flores-Montero, J., Kalina, T., Corral-Mateos, A., Sanoja-Flores, L., Pérez-Andrés, M., Martin-Ayuso, M., Sedek, L., Rejlova, K., Mayado, A., Fernández, P., van der Velden, V., Bottcher, S., van Dongen, J.J.M., Orfao, A., 2019. Fluorochrome choices for multicolor flow cytometry. J. Immunol. Methods. https://doi.org/10.1016/J.JIM.2019.06.009.

Fluxá Rodriguez, R., Orfao De Matos Correia E Valle, A., Hernández Herrero, J.B., 2017. Method of digital information classification. US 10, 133, 962 B2.

Fujikoshi, Y., Ulyanov, V.V., Shimizu, R., 2010. Multivariate Statistics: High-Dimensional and Large-Sample Approximations. Wiley-Blackwell, Oxford.

Futamura, K., Sekino, M., Hata, A., Ikebuchi, R., Nakanishi, Y., Egawa, G., Kabashima, K., Watanabe, T., Furuki, M., Tomura, M., 2015. Novel full-spectral flow cytometry with multiple spectrally-adjacent fluorescent proteins and fluorochromes and visualization of in vivo cellular movement. Cytometry A 87, 830–842. https://doi.org/10.1002/cyto.a.22725.

Heel, K., Tabone, T., Rohrig, K.J., Maslen, P.G., Meehan, K., Grimwade, L.F., Erber, W.N., 2013. Developments in the immunophenotypic analysis of haematological malignancies. Blood Rev. 27, 193–207. https://doi.org/10.1016/j.blre.2013.06.005.

Johansson, U., Bloxham, D., Couzens, S., Jesson, J., Morilla, R., Erber, W., Macey, M., British Committee for Standards in, H, 2014. Guidelines on the use of multicolour flow cytometry in the diagnosis of haematological neoplasms. British Committee for Standards in Haematology. Br. J. Haematol. 165, 455–488. https://doi.org/10.1111/bjh.12789.

Jolliffe, I.T., 2002. Principal Component Analysis, 2nd ed. Springer Series in Statistics Springer-Verlag New York, New York. https://doi.org/10.1007/b98835.

Kalina, T., Flores-Montero, J., van der Velden, V.H.J., Martin-Ayuso, M., Böttcher, S., Ritgen, M., Almeida, J., Lhermitte, L., Asnafi, V., Mendonça, a, de Tute, R., Cullen, M., Sedek, L., Vidriales, M.B., Pérez, J.J., te Marvelde, J.G., Mejstrikova, E., Hrusak, O., Szczepański, T., van Dongen, J.J.M., Orfao, a, 2012. EuroFlow standardization of flow cytometer instrument settings and immunophenotyping protocols. Leukemia 26, 1986–2010. https://doi.org/10.1038/leu.2012.122.

Leach, R.M., Drummond, M., Doig, A., 2013. Practical Flow Cytometry in Haematology Diagnosis. Wiley-Blackwell, Oxford. https://doi.org/10.1002/9781118487969.

Lhermitte, L., Mejstrikova, E., Van Der Sluijs-Gelling, A.J., Grigore, G.E., Sedek, L., Bras, A.E., Gaipa, G., Sobral Da Costa, E., Novakova, M., Sonneveld, E., Buracchi, C., De Sá Bacelar, T., Te Marvelde, J.G., Trinquand, A., Asnafi, V., Szczepanski, T., Matarraz, S., Lopez, A., Vidriales, B., Bulsa, J., Hrusak, O., Kalina, T., Lecrevisse, Q., Martin Ayuso, M., Brüggemann, M., Verde, J., Fernandez, P., Burgos, L., Paiva, B., Pedreira, C.E., Van Dongen, J.J.M., Orfao, A., Van Der Velden, V.H.J., 2018. Automated database-guided expert-supervised orientation for immunophenotypic diagnosis and classification of acute leukemia. Leukemia 32, 874–881. https://doi.org/10.1038/leu.2017.313.

Lucio, P., Parreira, A., van den Beemd, M.W., van Lochem, E.G., van Wering, E.R., Baars, E., Porwit-MacDonald, A., Bjorklund, E., Gaipa, G., Biondi, A., Orfao, A., Janossy, G., van Dongen, J.J., San Miguel, J.F., 1999. Flow cytometric analysis of normal B cell differentiation: a frame of reference for the detection of minimal residual disease in precursor-B-ALL. Leukemia 13, 419–427. https://doi.org/10.1038/sj.leu.2401279.

Lugli, E., Roederer, M., Cossarizza, A., 2010. Data analysis in flow cytometry: the future just started. Cytometry A 77, 705–713. https://doi.org/10.1002/cyto.a.20901.

Mair, F., Prlic, M., 2018. OMIP-044: 28-color immunophenotyping of the human dendritic cell compartment. Cytometry A 93, 402–405. https://doi.org/10.1002/cyto.a.23331.

Matarraz, S., Almeida, J., Flores-Montero, J., Lécrevisse, Q., Guerri, V., López, A., Bárrena, S., Van Der Velden, V.H.J., Te Marvelde, J.G., Van Dongen, J.J.M., Orfao, A., 2017. Introduction to the diagnosis and classification of monocytic-lineage leukemias by flow cytometry. Cytometry B Clin. Cytom. 92, 218–227. https://doi.org/10.1002/cyto.b.21219.

Meehan, S., Walther, G., Moore, W., Orlova, D., Meehan, C., Parks, D., Ghosn, E., Philips, M., Mitsunaga, E., Waters, J., Kantor, A., Okamura, R., Owumi, S., Yang, Y., Herzenberg, Leonard A., Herzenberg, Leonore A., 2014. AutoGate: automating analysis of flow cytometry data. Immunol. Res. 58, 218–223. https://doi.org/10.1007/s12026-014-8519-y.

Nováková, M., Glier, H., Brdičková, N., Vlková, M., Santos, A.H., Lima, M., Roussel, M., Flores-Montero, J., Szczepanski, T., Böttcher, S., van der Velden, V.H.J., Fernandez, P., Mejstříková, E., Burgos, L., Paiva, B., van Dongen, J.J.M., Orfao, A., Kalina, T., 2017. How to make usage of the standardized EuroFlow 8-color protocols possible for instruments of different manufacturers. J. Immunol. Methods. https://doi.org/10.1016/j.jim.2017.11.007.

O'Donnell, E.A., Ernst, D.N., Hingorani, R., 2013. Multiparameter flow cytometry: advances in high resolution analysis. Immune Netw. 13, 43. https://doi.org/10.4110/in.2013.13.2.43.

O'Gorman, M.R.G., Zollett, J., Bensen, N., 2011. Flow cytometry assays in primary immunodeficiency diseases. In: Hawley, T.S., Hawley, R.G. (Eds.), Flow Cytometry Protocols. Humana Press, Totowa, NJ, pp. 317–335. https://doi.org/10.1007/978-1-61737-950-5_15.

O'Neill, K., Aghaeepour, N., Špidlen, J., Brinkman, R., 2013. Flow cytometry bioinformatics. PLoS Comput. Biol. 9, e1003365. https://doi.org/10.1371/journal.pcbi.1003365.

Paiva, B., Merino, J., San Miguel, J.F., 2016. Utility of flow cytometry studies in the management of patients with multiple myeloma. Curr. Opin. Oncol. https://doi.org/10.1097/CCO.0000000000000331.

Pedreira, C.E., Costa, E.S., Arroyo, M.E., Almeida, J., Orfao, A., 2008a. A multidimensional classification approach for the automated analysis of flow cytometry data. IEEE Trans. Biomed. Eng. 55, 1155–1162. https://doi.org/10.1109/TBME.2008.915729.

Pedreira, C.E., Costa, E.S., Barrena, S., Lecrevisse, Q., Almeida, J., van Dongen, J.J., Orfao, A., EuroFlow, C., 2008b. Generation of flow cytometry data files with a potentially infinite number of dimensions. Cytometry A 73, 834–846. https://doi.org/10.1002/cyto.a.20608.

Pedreira, C.E., Costa, E.S., Lecrevisse, Q., van Dongen, J.J., Orfao, A., EuroFlow, C., 2013. Overview of clinical flow cytometry data analysis: recent advances and future challenges. Trends Biotechnol. 31, 415–425. https://doi.org/10.1016/j.tibtech.2013.04.008.

Pedreira, C., Elaine, S.E., Lecrevisse, Q., Grigore, G., Fluxá Rodriguez, R., Verde, J., Hernández, J., van Dongen, J.J.M., Orfao, A., 2019. From big flow cytometry datasets to smart diagnostic strategies: the EuroFlow approach. J. Immunol. Methods. https://doi.org/10.1016/j.jim.2019.07.003. 112631.

Perfetto, S.P., Chattopadhyay, P.K., Roederer, M., 2004. Seventeen-colour flow cytometry: unravelling the immune system. Nat. Rev. Immunol. 4, 648–655. https://doi.org/10.1038/nri1416.

Petrausch, U., Haley, D., Miller, W., Floyd, K., Urba, W.J., Walker, E., 2006. Polychromatic flow cytometry: a rapid method for the reduction and analysis of complex multiparameter data. Cytometry A 69, 1162–1173. https://doi.org/10.1002/cyto.a.20342.

Saeys, Y., Gassen, S.V., Lambrecht, B.N., 2016. Computational flow cytometry: helping to make sense of high-dimensional immunology data. Nat. Rev. Immunol. 16, 449–462. https://doi.org/10.1038/nri.2016.56.

Shearer, W.T., Rosenblatt, H.M., Gelman, R.S., Oyomopito, R., Plaeger, S., Stiehm, E.R., Wara, D.W., Douglas, S.D., Luzuriaga, K., McFarland, E.J., Yogev, R., Rathore, M.H., Levy, W., Graham, B.L., Spector, S.A., Pediatric AIDS Clinical Trials Group, 2003. Lymphocyte subsets in healthy children from birth through 18 years of age. J. Allergy Clin. Immunol. 112, 973–980. https://doi.org/10.1016/j.jaci.2003.07.003.

Staser, K.W., Eades, W., Choi, J., Karpova, D., DiPersio, J.F., 2018. OMIP-042: 21-color flow cytometry to comprehensively immunophenotype major lymphocyte and myeloid subsets in human peripheral blood. Cytometry A 93, 186–189. https://doi.org/10.1002/cyto.a.23303.

Swerdlow, S.H., Campo, E., Harris, N.L., Jaffe, E.S., Pileri, S.A., Stein, H., Thiele, J., Vardiman, J.W., 2008. WHO Classification of Tumours of Haematopoietic and Lymphoid Tissues, 4th ed. International Agency for Research on Cancer, Lyon.

Szczepanski, T., van der Velden, V.H., van Dongen, J.J., 2006. Flow-cytometric immunophenotyping of normal and malignant lymphocytes. Clin. Chem. Lab. Med. 44, 775–796. https://doi.org/10.1515/CCLM.2006.146.

Theunissen, P., Mejstrikova, E., Sedek, L., van der Sluijs-Gelling, A.J., Gaipa, G., Bartels, M., Sobral da Costa, E., Kotrová, M., Novakova, M., Sonneveld, E., Buracchi, C., 2016. Standardized flow cytometry for highly sensitive MRD measurements in B-cell acute lymphoblastic leukemia. Blood. https://doi.org/10.1182/blood-2016-07-726307.

Tung, J.W., Parks, D.R., Moore, W.A., Herzenberg, L.A., Herzenberg, L.A., 2004. New approaches to fluorescence compensation and visualization of FACS data. Clin. Immunol. 110, 277–283. https://doi.org/10.1016/j.clim.2003.11.016.

van der Burg, M., Kalina, T., Perez-Andres, M., Vlkova, M., Lopez-Granados, E., Blanco, E., Bonroy, C., Sousa, A.E., Kienzler, A.-K., Wentink, M., Mejstríková, E., Šinkorova, V., Stuchly, J., van Zelm, M.C., Orfao, A., van Dongen, J.J.M., 2019. The EuroFlow PID orientation tube for flow cytometric diagnostic screening of primary immunodeficiencies of the lymphoid system. Front. Immunol. 10, 246. https://doi.org/10.3389/fimmu.2019.00246.

van Dongen, J.J., Orfao, A., 2012. EuroFlow: resetting leukemia and lymphoma immunophenotyping. Basis for companion diagnostics and personalized medicine. Leukemia 26, 1899–1907. https://doi.org/10.1038/leu.2012.121leu2012121.

van Dongen, J.J.M., Lhermitte, L., Böttcher, S., Almeida, J., van der Velden, V.H.J., Flores-Montero, J., Rawstron, a, Asnafi, V., Lécrevisse, Q., Lucio, P., Mejstrikova, E., Szczepański, T., Kalina, T., de Tute, R., Brüggemann, M., Sedek, L., Cullen, M., Langerak, a W., Mendonça, a, Macintyre, E., Martin-Ayuso, M., Hrusak, O., Vidriales, M.B., Orfao, a, 2012. EuroFlow antibody panels for standardized n-dimensional flow cytometric immunophenotyping of normal, reactive and malignant leukocytes. Leukemia 26, 1908–1975. https://doi.org/10.1038/leu.2012.120.

van Dongen, J.J.M., van der Burg, M., Kalina, T., Perez-Andres, M., Mejstrikova, E., Vlkova, M., Lopez-Granados, E., Wentink, M., Kienzler, A.-K., Philippé, J., Sousa, A.E., van Zelm, M.C., Blanco, E., Orfao, A., 2019. EuroFlow-based flowcytometric diagnostic screening and classification of primary immunodeficiencies of the lymphoid system. Front. Immunol. 10, 1271. https://doi.org/10.3389/fimmu.2019.01271.

van Lochem, E.G., van der Velden, V.H., Wind, H.K., te Marvelde, J.G., Westerdaal, N.A., van Dongen, J.J., 2004. Immunophenotypic differentiation patterns of normal hematopoiesis in human bone marrow: reference patterns for age-related changes and disease-induced shifts. Cytometry B Clin. Cytom. 60, 1–13. https://doi.org/10.1002/cyto.b.20008.

Workgroup, I.I., 2013. Validation of cell-based fluorescence assays: practice guidelines from the International Council for Standardization of Haematology and International Clinical Cytometry Society. Cytometry B Clin. Cytom. 84, 281. https://doi.org/10.1002/cyto.b.21103.